

High-frequency electromagnetic properties of epitaxial $\text{Bi}_2\text{FeCrO}_6$ thin films grown by pulsed laser deposition

Brahim Aïssa,¹ Riad Nechache,^{2,3,a)} Daniel Therriault,⁴ Federico Rosei,³ and Mourad Nedil⁵

¹Smart Material and Sensors for Space Applications, MPB-Technologies, INC., 151 Hymus Boulevard, Montreal H9R 1E9, Canada

²NAST Center & Department of Chemical Science and Technology, University of Rome Tor Vergata Via della Ricerca Scientifica 1, 00133 Rome, Italy

³Centre Énergie, Matériaux et Télécommunications, INRS, 1650, boulevard Lionel-Boulet, Varennes, Québec J3X 1S2, Canada

⁴Center for Applied Research on Polymers (CREPEC), Mechanical Engineering Department, École Polytechnique de Montréal, PO Box 6079, Station "Centre-Ville," Montreal H3C 3A7, Canada

⁵UQAT (Université du Québec en Abitibi-Témiscamingue), laboratoire de recherche Télébec en communications souterraines, LRTCS, 450, 3e Avenue, Val-d'Or J9P 1S2, Canada

(Received 30 June 2011; accepted 12 October 2011; published online 4 November 2011)

We report on the electromagnetic (EM) properties in high-frequency domain (HF) of multiferroic $\text{Bi}_2\text{FeCrO}_6$ (BFCO) thin films. The films were epitaxially grown on SrTiO_3 substrates by pulsed laser ablation. Typical 50 nm-thick BFCO films having both (111) and (001) orientations were investigated. The films exhibit systematically deep EM absorbance narrow bands, localized in the HF X-band domain, with an attenuation reaching as high as $|-24|$ dB. The magnitude and the shape of EM absorption depend on the crystal orientation of the film. BFCO thin films show a promising potential for microwave application as specific frequency bands notch filters. © 2011 American Institute of Physics. [doi:10.1063/1.3657528]

The absorption and interference shielding of electromagnetic (EM) waves are important issues for commercial and military applications. The importance of electromagnetic interference (EMI) shielding has also increased in the last decade in the electronics and telecommunication industries due to widespread use of densely packed highly sensitive electronic devices.^{1,2} The technology is based on materials that can absorb EM radiation and convert it into heat or make EM waves vanish by interference.³ Recent increases in demand for faster, lighter, and more cost-efficient smart miniature devices operating in the GHz EM range,⁴ make some traditional thicker-microwave absorbing material (MAMs) too bulky to be useful in such small device designs. Therefore, the demands to develop thinner and more effective MAMs are ever increasing. Electromagnetic properties depend on magnetic or dielectric parameters such as permeability, permittivity, and loss constants.⁵ An efficient complementarity between these parameters, i.e., good EM match, is usually needed to achieve excellent (i.e., high reflection loss) EM absorption.⁶ Extensive investigations recently focused on developing materials with high EM matching, among which, carbon nanotubes CNTs/ CoFe_2O_4 ,⁷ and Ni(C) nanocapsules.⁸ Although these core-shell nanocomposites demonstrated a good EMI, their high density, low EM absorbance, and complex fabrication processes have hampered their integration in practical applications, such as stealth defense system.⁹

Multiferroic oxides, in which ferroelectricity and magnetic order coexist,¹⁰ possess tunable conductivity, making them promising candidates for microwave applications as thin film absorber materials. In addition, the film fabrication

process of these materials is well established and can be simply obtained by various techniques, including chemical vapour deposition (CVD), magnetron and radio-frequency sputtering, and pulsed laser deposition (PLD).

In this letter, we report on the microwave absorption properties of multiferroic $\text{Bi}_2\text{FeCrO}_6$ (BFCO) double perovskite films epitaxially grown on SrTiO_3 (STO) substrates. The observed high EM absorption of BFCO thin films in high-frequency domain (HF) represents an interesting alternative material for microwave related applications.

BFCO films were grown by PLD on (001) and (111)-oriented STO substrates as in Refs. 11 and 12. This leads to epitaxial and single phase BFCO films,¹³ as confirmed by x-ray diffraction (XRD) (cf. Fig. 1). In both cases, the $\theta - 2\theta$ XRD plots showed only reflections corresponding to the pseudocubic peaks from the 50 nm-thick BFCO films and STO substrates. The calculated out-of-plane c lattice parameters based on the pseudocubic structure were 3.962 Å. The in-plane pseudocubic parameters were estimated to be 3.906 Å, close to that of the STO substrate. Thus, the BFCO thin films crystallized in a distorted monoclinic structure with a large c/a ratio due to the strong in-plane compressive strain.

The recorded pattern for BFCO grown on STO (111) (cf. Fig. 1) revealed additional periodic superstructure peaks in the (111) direction. The latter is very intense, indicating good Fe/Cr cation ordering and high crystal quality BFCO thin films.

The EM properties of the BFCO films were characterized by using the coaxial transmission line method¹⁴ (Fig. 2(a)). To verify the EM-attenuation feature of the films, measurements of the EM energy transfer in a transition device were performed.¹⁵ The transition structure is characterized by a wide-band operating in the 1–16 GHz frequency range.¹⁶ To measure the transition scattering parameters, an Agilent

^{a)} Author to whom correspondence should be addressed. Electronic mail: nechache@emt.inrs.ca.

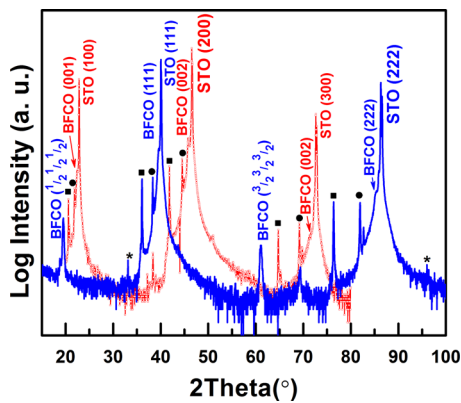


FIG. 1. (Color online) Structural characterization of (001) and (111)-oriented BFCO thin film. The squares correspond to K_{β} lines while the circles indicate contamination by tungsten of the x-ray tube cathode.

8722ES network analyzer was used. For each setup, transmission (S_{21}) and reflection (S_{11}) parameters were recorded with the network analyzer. The EM attenuation is deduced by comparing energy transmission between the two ports of the transition device in cases with and without measured samples.

Prior to EM shielding measurements, the frequency work band-pass (FWBP) of the system was determined by measuring the S_{11} of the reference samples. These reference samples consist of (1) the holder adapter (i.e., the transition device), (2) the naked STO substrate, and (3) substrates decorated with BFCO materials. The FWBP was then defined by the frequency range associated with S_{11} values below the $|-10|$ dB level.¹⁷

As a consequence, any measured EM shielding is known to be mainly due to the sole attenuation (S_{21}) of the sample being characterized. Figure 2(b) shows the measured (S_{11}) reflection coefficient for all the reference samples as a function of the EM frequency.

Hence, the FWBP of our system is corresponding to the 6–12 GHz range (i.e., X-band). On the other hand, all the reference samples exhibit a reflection coefficient of more than

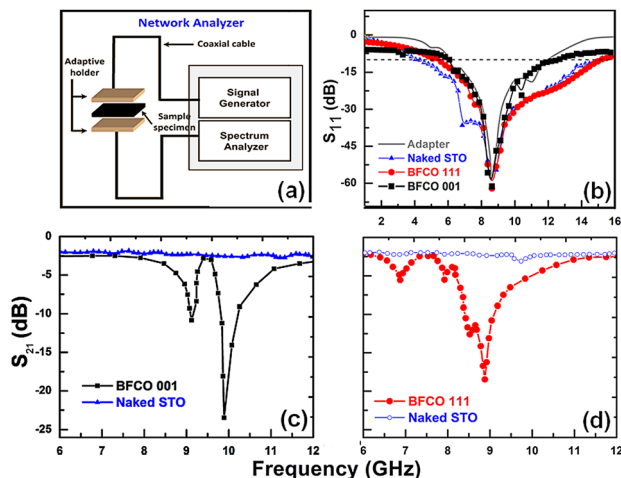


FIG. 2. (Color online) (a) Schematics of the coaxial transmission line method used to measure the electromagnetic shielding attenuation performance. (b) The reflection parameter (S_{11}) measured for the holder adapter, the naked STO substrate, and the grown (100) and (111) BFCO, respectively. EM absorption parameter (S_{21}) measured for the reference samples (i.e., holder adapter and naked STO substrate) and BFCO films (c) (001) and (d) (111) crystal orientations.

$|-60|$ dB around the 9 GHz frequency, meaning that less than 10^{-6} fraction of the incident EM Energy was reflected (i.e., practically, no EM reflection occurs at this frequency).

After the estimation of the FWBP, the EM absorption (and/or attenuation, (S_{21})) of the reference samples was systematically measured. As seen in Figures 2(c) and 2(d), the holder adapter and the naked STO substrates are almost transparent to EM radiation in the investigated frequency range. The rather weak and flat $|-2|$ dB measured for (S_{21}) is attributed to the thermal noise of the instrument and the experimental uncertainties. Deep and narrow EM-attenuation with a (S_{21}) reaching up to $|-18|$ dB around 9 GHz range is measured for (111)-oriented BFCO (cf. Fig. 2(c)). Weak attenuation of $|-5|$ dB is also observed at 7 GHz frequency band. (001)-oriented BFCO exhibit a deeper EM-attenuation of about $|-24|$ dB at 10 GHz. Additional attenuation of $|-11|$ dB can also be distinguished at around 9 GHz for BFCO (001). Since the STO substrate was shown to be almost transparent to EM radiation in the X-band, the measured EM attenuation is attributed to the BFCO thin film. This demonstrates that at the X-band frequency, the predominant EM attenuation mechanism in BFCO thin films is absorption rather than reflection.

In EM absorption, it is known that both electric and magnetic dipoles are strong absorbers of EM energy.^{18,19} For pure dielectric materials, such as ZnO (Ref. 20) and BaTiO₃,²¹ EM absorption is due to dielectric losses. In the case of pure magnetic materials, such as ferrites,²² the magnetic losses dominate over the dielectric losses. However, for multiferroic materials, the magnetic and dielectric losses should contribute equivalently to microwave absorption due to the combination of ferroelectricity and magnetic order.

To describe the significant EM absorption observed in the epitaxial grown BFCO thin films, we investigated their magnetic and ferroelectric properties. The magnetic properties were measured using a vibrating sample magnetometer with a sensitivity of 10^{-6} emu. The room temperature magnetic hysteresis loops of (001) and (111) oriented BFCO films are displayed in Fig. 3(a). The magnetic field H was applied in the plane of the films. The in-plane (IP) saturated magnetizations of BFCO were found to be 130 and 103 emu/cm³, corresponding to 1.6 and 1.3 μ_B /f.u., for (001) and (111) orientations, respectively.²³ The magnetization values of the BFCO films are slightly different between the two orientations.

Piezoresponse force microscopy (PFM)²⁴ was performed to probe the ferroelectric behavior of the BFCO films (Fig. 3(b)).²⁵ Local remanent piezoelectric hysteresis loops²⁶ observed for both orientations confirm the polarization switching and ferroelectric character of BFCO thin films. We also macroscopically measured the voltage dependence current density J in the films using an electroceramic analyzer (aixACCT TF Analyzer 2000). The (001)-oriented BFCO film shows leakage current densities of the order of 10^{-6} A/cm² in the zero electric field region, which is higher than the 10^{-7} A/cm² of BFCO film with (111) (cf. Fig. 3(c)). This may be attributed to high densities of crystal defects and oxygen vacancies and probably correlated with the ferroelectric domain wall morphology in the oriented films.²⁷

The maximum absorption of $|-24|$ dB at 10 GHz for the (001) oriented BFCO thin film is comparable with that of Fe/

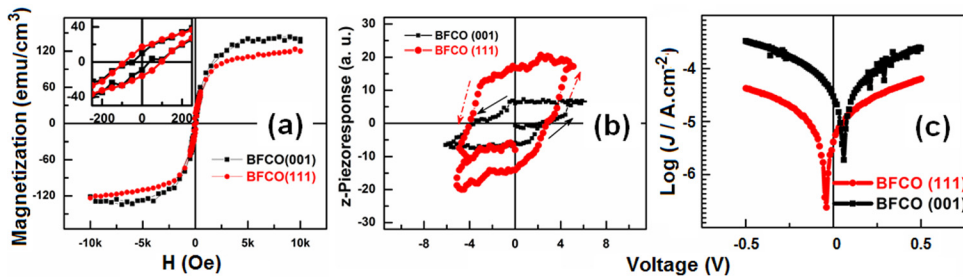


FIG. 3. (Color online) Multiferroic properties of epitaxial BFCO thin films: (a) Room temperature magnetization hysteresis of (001) and (111)-oriented BFCO films and their corresponding (b) ferroelectric hysteresis loops, and (c) voltage dependence current density J .

CNTs (more than -25 dB)²⁸ and CNTs/CoFe₂O₄ (-18 dB).⁵ The better microwave absorption properties observed in BFCO (001) can be attributed to the enhancement of magnetization and leakage current density in the films. Domain walls could behave as a pathway through which electrical conduction can occur and thereby contributes to the EM attenuation.

In summary, we demonstrated a significant EM attenuation, as high as $|-24|$ dB in the HF X-band domain, of multiferroic BFCO epitaxial thin films grown by PLD. This effect exciting result is attributed to the perfect EM matching originating from the coexistence of ferroelectric and magnetic order in the films. The observed high EM absorption of BFCO films is promising for microwave applications, such as specific frequency bands notch filters.²⁹ Further investigations are under way to determine in detail the effect of cation ordering and ferroelectric domain walls on the EM absorption pattern of BFCO epitaxial films as well as BFCO submicron and nanostructures.¹¹

We acknowledge financial support from the Canada Foundation for Innovation. F. R. and M. N. are supported by NSERC and FQRNT grants. F.R. is grateful to the Canada Research Chairs Program for partial salary support and to MDEIE for an international collaboration grant with the University of Rome “Tor Vergata”. The authors thank L.-P. Carignan and D. Menard (École Polytechnique Montreal) for technical support in the magnetic measurements. R.N. is grateful to the joint laboratory on Advanced Materials for Energy, Environment and Health, University of Rome «Tor Vergata» for partial salary support. Brahim Aïssa and Riad Nechache contributed equally to this work.

¹T. W. Kang and Y. C. Jeong, Real-Time Embedded World (Korean magazine), **6**, 49 (2000).

²K. Y. Park, S. E. Lee, C. G. Kim, and J. H. Han, *Compos. Sci. Technol.* **66**, 576 (2006).

³S. Kimura, T. Kato, T. Hyodo, Y. Shimizu, and M. Egashira, *J. Magn. Magn. Mater.* **312**, 181 (2007).

⁴A. N. Yusoff and M. H. Abdulla, *J. Magn. Magn. Mater.* **269**, 271 (2004).

⁵T. F. Zhang, M. S. Cao, and J. Yuan, *J. Aeronaut. Mater.* **62**, 46 (2001).

⁶A. Wadhawan, D. Garrett, and J. M. Perez, *Appl. Phys. Lett.* **83**, 2683 (2003).

⁷R. C. Che, C. Y. Zhi, C. Y. Liang, and X. G. Zhou, *Appl. Phys. Lett.* **88**, 033105 (2006).

⁸X. F. Zhang, X. L. Dong, H. Huang, Y. Y. Liu, W. N. Wang, X. G. Zhu, B. Lev, J. P. Lei, and C. G. Lee, *Appl. Phys. Lett.* **89**, 053115 (2006).

⁹Y. H. Zou, H. B. Liu, L. Yang, and Z. Z. Chen, *J. Magn. Magn. Mater.* **302**, 343 (2006).

¹⁰N. A. Spaldin and M. Fiebig, *Science* **309**, 391 (2005).

¹¹R. Nechache, C. Harnagea, A. Pignolet, F. Normandin, T. Veres, L.-P. Carignan, and D. Menard, *Appl. Phys. Lett.* **89**, 102902 (2006).

¹²R. Nechache, C. V. Cojocaru, C. Harnagea, C. Nauenheim, M. Nicklaus A. Ruediger, F. Rosei, and A. Pignolet, *Adv. Mater.* **23**, 1724 (2011).

¹³R. Nechache, C. Harnagea, L.-P. Carignan, O. Gautreau, L. Pintilie, M. P. Singh, D. Menard, P. Fournier, M. Alexe, and A. Pignolet, *J. Appl. Phys.* **105**, 061621 (2009).

¹⁴B. Aïssa, L. L. Laberge, M. A. Habib, T. A. Denidni, D. Therriault, and M. A. El Khakani, *J. Appl. Phys.* **109**, 084313 (2011).

¹⁵The mentioned transition uses the EM coupling through a slot etched in a common ground plane between two ports, one based on conductor backed coplanar waveguide technology and another based on micro-strip technology.

¹⁶M. Nedil, T. A. Denidni, and A. Djaiz, *Electron. Lett.* **43**, 464 (2007).

¹⁷This level means that more than 90% of the EM energy is transmitted from the holder adapter to the samples specimen under test.

¹⁸H. F. Zhang, S. W. Or, and H. J. W. Chan, *J. Appl. Phys.* **104**, 104109 (2008).

¹⁹G. Alvarez, H. Montiel, M. A. Castellanos, J. Heiras, and R. Valenzuela, *Mater. Sci. Eng. B* **150**, 175 (2008).

²⁰R. F. Zhuo, L. Qiao, H. T. Feng, J. T. Chen, D. Yan, Z. G. Wu, and P. X. Yan, *J. Appl. Phys.* **104**, 094101 (2008).

²¹S. M. Abbas, A. K. Dixit, R. Chatterjee, and T. C. Goel, *Mater. Sci. Eng. B* **123**, 167 (2005).

²²J. Smit and H. P. J. Wijn, *Ferrites* (Philips Technical Library, Eindhoven, 1959), p. 273.

²³The noticeable magnetizations are due to the presence of high Fe/Cr cation ordering, which allows the superexchange magnetic interaction between the two cations via oxygen ions.

²⁴R. Nechache, C. Harnagea, A. Ruediger, F. Rosei, and A. Pignolet, *Funct. Mater. Lett.* **3**, 83 (2010).

²⁵This technique probes the ferroelectric or piezoelectric nature of polar films and nanostructures with a resolution in the tens of nm range.

²⁶C. Harnagea, A. Pignolet, M. Alexe, D. Hesse, and U. Goesele, *Appl. Phys. A* **71**, 261 (2000).

²⁷J. Seidel, L. W. Martin, Q. He, Q. Zhan, Y. H. Chu, A. Rother, M. E. Hawkrige, P. Maksymovych, P. Yu, M. Gajek, N. Balke, S. V. Kalinin, S. Gemming, F. Wang, G. Catalan, J. F. Scott, N. A. Spaldin, J. Orenstein, and R. Ramesh, *Nature Mater.* **8**, 229 (2009).

²⁸R. C. Che, L. M. Peng, X. F. Duan, Q. Chen, and X. L. Liang, *Adv. Mater.* **16**, 401 (2004).

²⁹Notch filter is a filter that eliminates a single frequency or narrow band of frequencies. This filter is commonly used in electronics for signal processing. Narrow EM absorption band and high attenuation observed in BFCO thin films can help, for example, to design simple and compact optical systems for optical applications, such as thin film filters for Raman spectroscopy.